AFRL-RW-EG-TP-2012-003

Shock Equation of State of Multi-Constituent Epoxy-Metal Particulate Composites

Jennifer L. Jordan[1]
Eric B. Herbold[2]
Gerrit Sutherland[3]
Andrew Frazer[4]
John Borg[4]
D. Wayne Richards[1]

[1]Air Force Research Laboratory, AFRL/RW, Eglin AFB, FL 32542
[2]School of Materials Science and Engineering, Georgia Institute of Engineering, Atlanta, GA 30332
[3]Naval Surface Warfare Center, Indian Head, MD 20640
[4]Department of Mechanical Engineering, Marquette Univ, Milwaukee, WI 53233

May 2012

Interim Report

AIR FORCE RESEARCH LABORATORY, MUNITIONS DIRECTORATE

Air Force Materiel Command ■ United States Air Force ■ Eglin Air Force Base

NOTICE AND SIGNATURE PAGE

Using Government drawings, specifications, or other data included in this document for any purpose other than Government procurement does not in any way obligate the U.S. Government. The fact that the Government formulated or supplied the drawings, specifications, or other data does not license the holder or any other person or corporation; or convey any rights or permission to manufacture, use, or sell any patented invention that may relate to them.

Qualified requestors may obtain copies of this report from the Defense Technical Information Center (DTIC) (http://www.dtic.mil).

AFRL-RW-EG-TP-2012-003 HAS BEEN REVIEWED AND IS APPROVED FOR PUBLICATION IN ACCORDANCE WITH ASSIGNED DISTRIBUTION STATEMENT.

FOR THE DIRECTOR:

WHITE.HOWARD.G.1230779062
Digitally signed by WHITE.HOWARD.G.1230779062
DN: c=US, o=U.S. Government, ou=DoD, ou=PKI, ou=USAF, cn=WHITE.HOWARD.G.1230779062
Date: 2012.05.08 10:16:37 -05'00'

HOWARD G. WHITE, PhD
Technical Advisor
Ordnance Division

VARNER.CHRISTOPHER.L.1265664543
Digitally signed by VARNER.CHRISTOPHER.L.1265664543
DN: c=US, o=U.S. Government, ou=DoD, ou=PKI, ou=USAF, cn=VARNER.CHRISTOPHER.L.1265664543
Date: 2012.05.01 08:31:10 -05'00'

CHRISTOPHER L. VARNER
Branch Chief
Energetic Materials Branch

JORDAN.JENNIFER.L.1265297915
Digitally signed by JORDAN.JENNIFER.L.1265297915
DN: c=US, o=U.S. Government, ou=DoD, ou=PKI, ou=USAF, cn=JORDAN.JENNIFER.L.1265297915
Date: 2012.05.01 08:23:08 -05'00'

JENNIFER L. JORDAN, PhD
Project Manager
Energetic Materials Branch

This report is published in the interest of scientific and technical information exchange, and its publication does not constitute the Government's approval or disapproval of its ideas or findings.

This page intentionally left blank

REPORT DOCUMENTATION PAGE

Form Approved
OMB No. 0704-0188

1. REPORT DATE *(DD-MM-YYYY)*	**2. REPORT TYPE**	**3. DATES COVERED** *(From - To)*
05-2012	Interim	October 2009 – July 2010

4. TITLE AND SUBTITLE

Shock Equation of State of Multi-Constituent Epoxy-Metal Particulate Composites

5a. CONTRACT NUMBER

5b. GRANT NUMBER

5c. PROGRAM ELEMENT NUMBER
62102F

6. AUTHOR(S)

Jennifer L. Jordan[1], Eric B. Herbold[2], Gerrit Sutherland[3], Andrew Frazer4, John Borg[4], D. Wayne Richards[1]

5d. PROJECT NUMBER
4347

5e. TASK NUMBER
95

5f. WORK UNIT NUMBER
05

7. PERFORMING ORGANIZATION NAME(S) AND ADDRESS(ES)

[1]Air Force Research Laboratory, AFRL/RW, Eglin AFB, FL 32542
[2]School of Materials Science and Engineering, Georgia Institute of Engineering, Atlanta, GA 30332
[3]Naval Surface Warfare Center, Indian Head, MD 20640
[4]Department of Mechanical Engineering, Marquette Univ, Milwaukee, WI 53233

8. PERFORMING ORGANIZATION REPORT NUMBER

AFRL-RW-EG-TP-2012-003

9. SPONSORING / MONITORING AGENCY NAME(S) AND ADDRESS(ES)

Air Force Research Laboratory, Munitions Directorate
Ordnance Division
Energetic Materials Branch (AFRL/RWME)
Eglin AFB FL 32542-5910
Technical Advisor: Dr. Jennifer L. Jordan

10. SPONSOR/MONITOR'S ACRONYM(S)
AFRL-RW-EG

11. SPONSOR/MONITOR'S REPORT NUMBER(S)
AFRL-RW-EG-TP-2012-003

12. DISTRIBUTION / AVAILABILITY STATEMENT

Distribution A: Approved for public release; distribution unlimited. Approval Confirmation 96 ABW/PA # 96ABW-2010-0398, Dated July 7, 2010

13. SUPPLEMENTARY NOTES

DISTRIBUTION STATEMENT INDICATING AUTHORIZED ACCESS IS ON THE COVER PAGE AND BLOCK 12 OF THIS FORM.

14. ABSTRACT

The shock properties of epoxy-based particulate composites have been extensively studied in the literature. Generally, these materials only have a single particulate phase; typically alumina. This paper presents equation of state experiments conducted on five epoxy-based particulate composites. The shock stress and shock velocity states were measured for five different composites: two epoxy-aluminum two-phase composites, with various amounts of aluminum, and three epoxy-aluminum-metal composites, where the metal constituent was either copper, nickel, or tungsten. The impact velocities ranged from 300 to 960 m/s. Numerical simulations of the experiments of epoxy-Al are compared with mesoscale simulations of epoxy-Al_2O_3 composites to investigate the effect of the soft versus hard particulate; additionally, an epoxy-Al–W simulation was conducted to investigate the material properties of the second phase on shock response of these materials. In these epoxy-based particulate composites, the slope of the shock velocity-particle velocity curve appears to depend on the epoxy binder. It is shown that the addition of only 10 vol % of a second, denser metallic phase significantly affects the shock response in these composites.

15. SUBJECT TERMS
Particulate composite, epoxy, Hugoniot, shock

16. SECURITY CLASSIFICATION OF:			**17. LIMITATION OF ABSTRACT**	**18. NUMBER OF PAGES**	**19a. NAME OF RESPONSIBLE PERSON**
a. REPORT	**b. ABSTRACT**	**c. THIS PAGE**			Jennifer L. Jordan
UNCLASSIFIED	UNCLASSIFIED	UNCLASSIFIED	UL	15	**19b. TELEPHONE NUMBER** *(include area code)* 850-882-8992

Standard Form 298 (Rev. 8-98)
Prescribed by ANSI Std. Z39.18

This page intentionally left blank

Shock equation of state of multi-constituent epoxy-metal particulate composites

Jennifer L. Jordan,[1,a)] Eric B. Herbold,[2] Gerrit Sutherland,[3] Andrew Fraser,[4] John Borg,[4] and D. Wayne Richards[1]
[1]*Air Force Research Laboratory, AFRL/RW, Eglin AFB, Florida 32542, USA*
[2]*School of Materials Science and Engineering, Georgia Institute of Technology, Atlanta, Georgia 30332, USA*
[3]*Naval Surface Warfare Center, Indian Head, Maryland 20640, USA*
[4]*Department of Mechanical Engineering, Marquette University, Milwaukee, Wisconsin 53233, USA*

(Received 15 July 2010; accepted 29 November 2010; published online 14 January 2011)

The shock properties of epoxy-based particulate composites have been extensively studied in the literature. Generally, these materials only have a single particulate phase; typically alumina. This paper presents equation of state experiments conducted on five epoxy-based particulate composites. The shock stress and shock velocity states were measured for five different composites: two epoxy-aluminum two-phase composites, with various amounts of aluminum, and three epoxy-aluminum-(metal) composites, where the metal constituent was either copper, nickel, or tungsten. The impact velocities ranged from 300 to 960 m/s. Numerical simulations of the experiments of epoxy-Al are compared with mesoscale simulations of epoxy-Al_2O_3 composites to investigate the effect of the soft versus hard particulate; additionally, an epoxy-Al–W simulation was conducted to investigate the material properties of the second phase on shock response of these materials. In these epoxy-based particulate composites, the slope of the shock velocity-particle velocity curve appears to depend on the epoxy binder. It is shown that the addition of only 10 vol % of a second, denser metallic phase significantly affects the shock response in these composites.
 [doi:10.1063/1.3531579]

I. INTRODUCTION

Particulate composites comprised of a polymer binder with one or multiple particulate phases have a variety of engineering applications with their high strength and low density. The shock properties of such composites are of interest as explosives and propellants are composed of particulate phases in polymer binders. There are several studies in the literature regarding the equation of state of single particulate based epoxy-Al_2O_3 (Refs. 1–5) and epoxy-WC (Ref. 6) composites. Although these single component systems interact in a complex manner with shock waves, the addition of a second metal or ceramic particulate, such as in epoxy-Al–Fe_2O_3 (Refs. 7 and 8) or epoxy-Al–MnO_2,[9,10] can result in even more complex interactions. The propagated wave observed in epoxy-Al_2O_3 broadens at low input stress due to the increased time available for viscous mechanisms.[5] As the input stress increases, the epoxy-Al_2O_3 composite material exhibits viscoelastic behavior.[3] Additionally, the release wave velocity is a strong function of particle velocity and much faster than the initial shock wave.[2,5] A recent investigation shows that epoxy-WC composites have a similar stress-strain response as epoxy-Al_2O_3 composites, as well as a strong dependence of release wave speed on particle velocity.[6]

In epoxy,[11–13] Carter and Marsh[11] observed failure of the shock velocity to extrapolate to the ultrasonic bulk sound speed, which they attributed to the compressed distance between the polymer chains with rigid polymer backbones. Additionally, they observe a high pressure phase transition, at ~23 GPa, which was attributed to interchain chemical reactions.[11]

This paper will discuss equation of state experiments conducted on epoxy-based particulate composites. These composites contain aluminum powder, for two-phase composites, along with copper, nickel, or tungsten powder, for three phase composites. It has been shown that the matrix material dominates the bulk shock response of epoxy-based particulate composites regardless of the material properties of the particulate phase.[4–6] The third phase here is added to investigate the effects of the complementary deformation of the two powder phases. For example, it was shown in Ref. 14 that the addition of a hard and/or dense third phase changes the distribution of internal energy in shocked three phase composites. Stress and time of arrival were measured using manganin gauges. The effect of the deformability of the particulate is investigated through simulations of the epoxy-Al composite studied in this paper with the epoxy-Al_2O_3 composite extensively studied in the literature. The addition of a second particulate phase is considered through simulations of the epoxy-Al–W composite.

II. EXPERIMENTAL PROCEDURE

Five materials were prepared for this study—two composites containing only epoxy and aluminum, at two volume fractions, and three composites containing the addition of a second metallic phase. The manufacturer and average par-

[a)]Electronic mail: jennifer.jordan@eglin.af.mil.

TABLE I. Particulate characteristics.

Powder	Supplier	Average particle size (μm)
Aluminum (X81)	Toyal	27
Copper	Atlantic equipment engineers	37
Nickel	Atlantic equipment engineers	44
Tungsten[a]	H. C. Starck (Kulite)	37

[a]Reference 15.

ticle size for the powders are given in Table I. The appropriate volume fractions of powder for each composite were blended into Epon 826 and cured with diethanolamine. The composite mixture was cast into blocks and nominally 34.9 mm diameter by 3.2 mm thick samples were machined. The density of each composite was measured using pyncnometry. The longitudinal and shear ultrasonic wave speeds in the composites were measured using a GE Panametrics 25 HP Plus ultrasonic thickness gauge with a 2.25 MHz M106 transducer for longitudinal measurements and a 2.25 MHz V154 transducer for shear measurements. The compositions of all the materials, along with their measured densities and sound speeds, are given in Table II. Micrographs of each of the composites are given in Figs. 1(a)–1(e).

Four gas gun-driven equation of state experiments, with impact velocities ranging from 300 to 960 m/s, were conducted using the 102 mm diameter single-stage light-gas gun at NSWC-Indian Head. The test configuration[9] used in this study allows for the simultaneous measurement of three samples. Each sample was instrumented with two 50 Ω manganin gauge (Dynasen, Goleta, CA), which have an active gauge area of 40.3 mm^2 and a nominal thickness of 0.05 mm, mounted between the donor plate and the sample and between two sample disks. An aluminum projectile with an aluminum flyer plate (12.7 mm nominal thickness) was used to impact an aluminum driver plate (6.73 mm nominal thickness) with the samples mounted on the rear of the driver plate. All of the plates were machined from 6061-T6 Al. The gauge mounted between the driver and the sample provides and "input" stress profile, and the gauge mounted between the two sample disks provides the "transmitted" stress profile.

III. RESULTS AND DISCUSSION

Three impact velocities were used to determine the response of these epoxy-based particulate composites to shock loading. epoxy-45Al and epoxy-Al–W were impacted at 302 m/s. All the samples were impacted at the identical impact condition of 620 m/s, and epoxy-45Al was also impacted at 960 m/s.

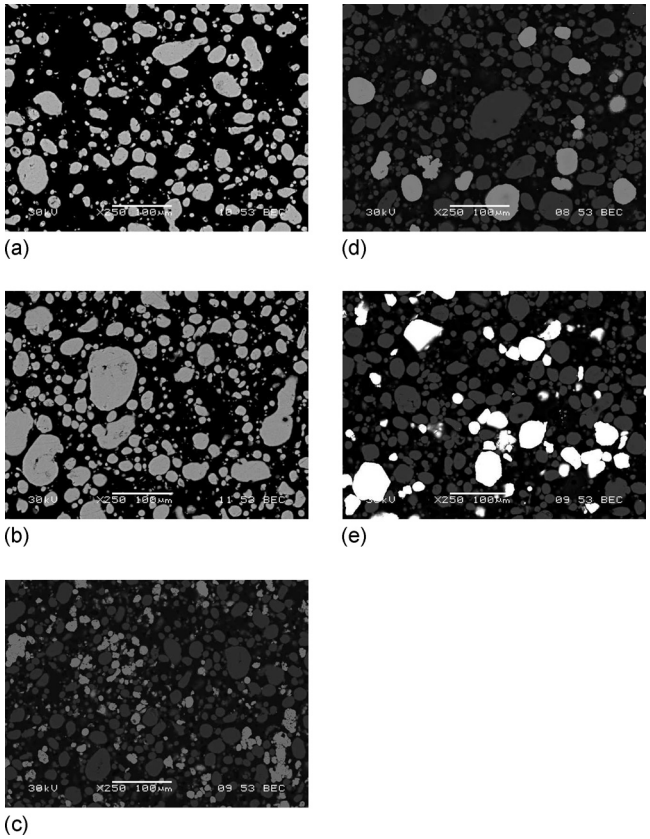

FIG. 1. Micrographs of (a) epoxy-35Al, where the light gray particles are aluminum; (b) epoxy-45Al, where the light gray particles are aluminum; (c) epoxy-Al–Cu, where the light gray particles are copper and the dark gray particles are aluminum; (d) epoxy-Al–Ni, where the light gray particles are nickel and the dark gray particles are nickel; and (e) epoxy-Al–W, where the white particles are tungsten and the dark gray particles are aluminum.

The transmitted pressure pulses for each sample at 622–624 m/s impact velocity are shown in Fig. 2. The large spikes in the epoxy-Al–Cu and epoxy-Al–Ni traces are due to failure of the input gauge. The regular oscillations on several wave profiles appear to be due to electronic noise rather than oscillations within the gauge package. There is little observable difference in the wave profiles between samples, other than the magnitude, which may be explained through the measured density differences of the materials. The wave profiles show rounding at the peak of the rise indicating

TABLE II. Material compositions, measured densities, and measured longitudinal (C_L) and shear (C_S) sound speeds, and calculated bulk sound speed (C_b).

Material	Density (g/cm^3)	C_L (km/s)	C_S (km/s)	C_b (km/s)	Al (vol %)	Cu (vol %)	Ni (vol %)	W (vol %)	epoxy (vol %)
Epoxy-35Al	1.725	2.95	1.49	2.40	35				65
Epoxy-45Al	1.875	3.13	1.61	2.52	45				55
Epoxy-Al–Cu	2.475	2.77	1.40	2.25	35	10			55
Epoxy-Al–Ni	2.513	2.95	1.49	2.40	35		10		55
Epoxy-Al–W	3.652	2.39	1.20	1.95	35			10	55

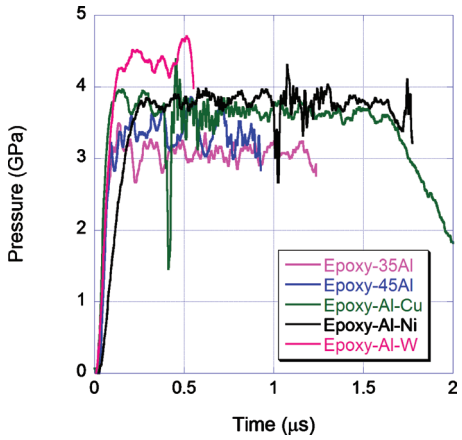

FIG. 2. (Color) Transmitted pressure vs time traces for all samples at 622 m/s impact velocity.

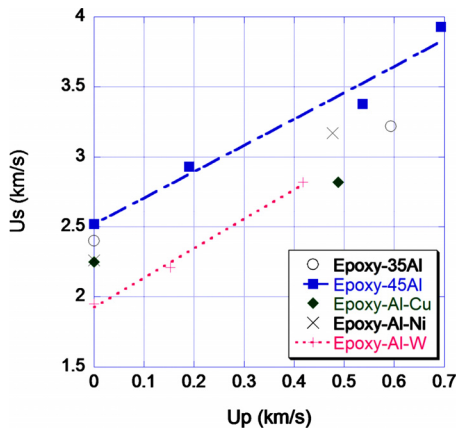

FIG. 3. (Color online) Shock velocity vs particle velocity for all experiments.

dispersion.[5] However, the wave dispersion does not appear to depend on the presence or type of the second phase in the material.

In each experiment, the shock velocity (U_s), shown in Table III, was determined from the difference between the time of arrival at the manganin gauge mounted between the donor plate and the sample and the gauge mounted between the two samples and the known sample thickness. The pressure in each sample was determined at an input and a transmitted location, approximately 3.2 mm apart, by averaging the pressure at the plateau observed in the manganin gauge signals. These measured pressures are also presented in Table III as P_{in} and P_{out}, respectively. In several experiments, it appears that the transmitted pressure is higher than the input pressure, which is physically impossible. The error on these average measurements is approximately 10%, which equates to the input and propagated pressures being equal. The particle velocity, u_p, was determined using the measured shock velocities and input pressure for each experiment by the conservation equation

$$P = \rho_0 U_s u_p, \tag{1}$$

where ρ_0 is the initial density. For experiments where the input pressure was not measured, the transmitted pressure was used, which is valid based on the experiments where both pressures were measured showing a steady wave over the 3.2 mm propagation distance.

The shock velocity versus particle velocity for each of the samples is given in Fig. 3. An empirical linear equation of state can be fit in the $U_s - u_p$ space

$$U_s = C_0 + s u_p, \tag{2}$$

where C_0 is the bulk sound speed in the material at zero pressure and s is an empirical parameter. For the epoxy-45Al sample, the shock velocity was measured at three particle velocities, in addition to the bulk sound speed measured using ultrasound, and a least-squares linear fit determined

$$U_s = 2.52 + 1.89 u_p. \tag{3}$$

Although only two points were measured for epoxy-Al–W, a similar linear fit, with the measured ultrasonic bulk sound speed, was constructed resulting in

$$U_s = 1.92 + 2.11 u_p, \tag{4}$$

which may be compared to the fit of the epoxy-WC composite with 46 vol % WC from Ref. 6 which was $U_s = 1.65 + 2.15 u_p$. It is interesting that epoxy-45Al and epoxy-Al–W have similar behavior to composites in the literature,[4–6] as seen in Fig. 4. The shock velocity-particle velocity lines are parallel within approximately 10% of each other. This indicates that the epoxy binder is driving the shock response of these materials, with small variations in the epoxy resins and curing agents possibly accounting for the 10% difference.

TABLE III. Experimental results for gas gun experiments on epoxy-based particulate composites, where U_s is the shock velocity, P_{in} is the pressure from the input manganin gauge, P_{out} is the pressure from the transmitted manganin gauge, and u_p is the calculated particle velocity.

Sample	Impact velocity (m/s)	U_s (km/s)	P_{in} (GPa)	P_{out} (GPa)	u_p (km/s)
Epoxy-35Al	622 ± 8	3.22	3.3	3.1	0.593
Epoxy-45Al	302 ± 2	2.93	1.05	1.04	0.190
Epoxy-45Al	622 ± 8	3.38		3.4	0.537
Epoxy-45Al	960 ± 2	3.93		5.1	0.693
Epoxy-Al–Cu	624 ± 0.5	3.03	3.4	3.6	0.488
Epoxy-Al–Ni	624 ± 0.5	3.17		3.8	0.477
Epoxy-Al–W	302 ± 2	2.21	1.2	1.3	0.153
Epoxy-Al–W	624 ± 0.5	2.82	4.3	4.4	0.418

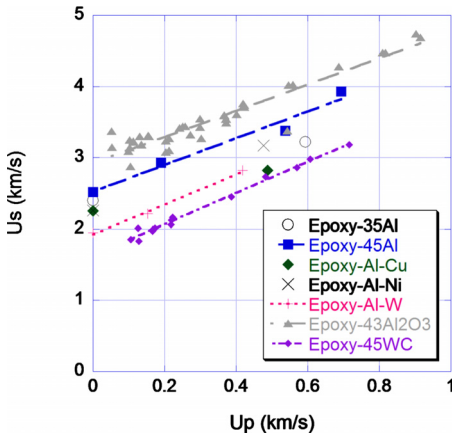

FIG. 4. (Color online) Shock velocity vs particle velocity for all experiments compared with literature data for epoxy-43 vol % Al_2O_3 (Refs. 2–5) and epoxy-WC (Ref. 6).

For the materials presented here, the total volume fraction of particulate is the same in epoxy-45Al and the epoxy-Al-(metal) composites, with epoxy-35Al containing the same volume fraction of aluminum as the epoxy-Al-(metal) samples and 10 vol % less aluminum than epoxy-45Al. For epoxy-45Al and epoxy-Al–W, the ultrasonically measured sound speed appears to be linear with the measured $U_s - u_p$ data points. In polymers, the extrapolated C_0 value, from a linear fit to the experimental shock-loading points, is typically higher than the ultrasonically measured bulk sound speed.[11] However, Millett *et al.*[4] observed that this behavior shifted to the more common behavior of the extrapolated C_0 correlating with the ultrasonically measured bulk sound speed with increasing amounts of alumina, which is observed in these materials.

Millettt *et al.*[4] also observed that the slope, s, appears to be controlled by the epoxy binder, since there was little difference in the slopes of two alumina-epoxy composites with different volume fractions of alumina. Despite the limited data in this study, this also appears to be true for these epoxy-based composites. The s values in Eqs. (1) and (2) are higher than those reported by Carter and Marsh (1.51),[11] Munson and May (1.66),[12] and Millett *et al.* (1.47) (Ref. 13) for the pure epoxy resin. The small differences between the reported literature values are likely due to differences in hardeners and plasticizers used to cure the epoxy resin. Additionally, Setchell and Anderson[3] report $s=2.00$ for 43 vol % Al_2O_3 and Millett *et al.*[4] report values of $S=1.63$ for their "fully loaded" alumina-epoxy composite and $s=1.66$ for the "half loaded" composite. An average value of s fit to all the epoxy-43 vol % Al_2O_3 data[2–5] is 1.84, as shown in Fig. 3. The slopes of all the epoxy-based composites, with the epoxy-43 vol % Al_2O_3 composite showing a shallower slope than epoxy-45Al, epoxy-Al–W, and epoxy-WC.

IV. NUMERICAL MODELING

Numerical simulations of the shock response of epoxy-Al composites, considered in this study, are presented and contrasted with simulations using epoxy-Al_2O_3, which has been studied extensively in the literature, to investigate the effects of material properties and particle morphology of the powder within the matrix. Results of three component systems using epoxy-Al–W for comparison with Eq. (4) and to investigate the effects of adding only 10% of third, dense material in numerical simulations are also presented.

The two-dimensional microstructural images [similar to Fig. 1(b)] are converted into vectorized lists of particle boundaries for the simulated impact of the domain. Many investigations use randomly distributed circles, squares and cubes with appropriate size and distribution to represent powder particles in mesoscale simulations[6,14–17] with excellent results. The fine details of the particle surface are usually not as important as nominal aspect ratio (e.g., nominally round or flat[18]) and the size distribution due to the fact that small asperities on the particle surfaces may be diminished in the advection step in hydrocodes. The use of digitized micrographs does indicate the nominal shape and size distribution, but the intended volume (area) fraction of constituents must be verified to account for the fact that micrographs are a two-dimensional representation of a three-dimensional material. Thus, the resulting digitization is highly dependent on the precise location of the polished reference surface.

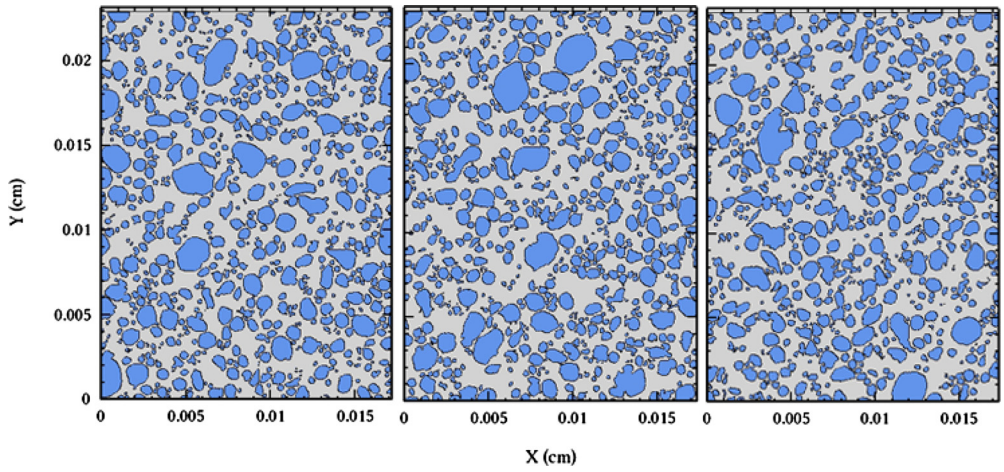

FIG. 5. (Color online) Initial vectorized microstructures for simulation of experiments with epoxy-45Al.

TABLE IV. Calculated volume fraction and density of digitized microstructures for numerical simulations for epoxy-45Al and epoxy-Al–W.

Material	Designation	Volume fraction epoxy	Volume fraction Al	Volume fraction W	ρ_0 (g/cc)
Epoxy-45Al	Microstructure A	52.8	47.2	0	1.876
Epoxy-45Al	Microstructure B	51.8	48.2	0	1.892
Epoxy-45Al	Microstructure C	53.1	46.9	0	1.872
Epoxy-Al–W	Microstructure D	58.3	29.1	12.6	3.877

A custom MATLAB program was used to threshold the grayscale values of the particles, separate the phases within the composite and locate the boundaries. The outline of the particles was then converted to a vector list representation and scaled from a pixel to length scale (similar to Ref. 18). The program created an input file for each specific simulation for a parallel version of CTH, which is a finite volume three-dimensional shock wave physics code.[19]

The two-dimensional microstructures used in the shock-loading simulations are shown in Figs. 5(a)–5(c), 7, and 8(a). The microstructures were discretized into 0.36 μm cells in Figs. 5 and 8 and 0.06 μm cells in Fig. 7. The top and bottom boundaries are given transmitting boundary conditions. The sides of the computational domain are prescribed as symmetry planes. The calculated volume fractions and densities are given in Table IV. The three digitized microstructures in Fig. 5 were each impacted at 302, 622, and 960 m/s (as shown in Table III) by a 6061-T6 Al half-space placed above the sample to produce an infinitely long shock.

The sizes of the micrographs were selected based upon simulations (not shown) where multiple microstructures were stitched together to lengthen the sample in the direction of the shock. The measured difference between the shock and particle velocity was within the difference (<1%) observed by changing the location of the line of tracers and using different digitized microstructures.

To measure the shock velocity and particle velocity for comparison with experiments, a horizontal line of 150 tracer particles is placed within the composite at $y=0.002$ cm and $y=0.022$ cm similar to the methods in Refs. 6 and 20–22. The shock speed was calculated by determining the time when the pressure of each tracer particle reached half of its maximum height. The shock speed is then calculated using the position and the "half-maximum" of pressure times of the tracers that were initially above and below one another. All of the individual speeds are then averaged together resulting in a single shock speed for the simulation. The particle speed is determined by taking the average particle speed in the direction of the shock of the tracer particles after the shock has passed.

The results from these simulations are shown in Fig. 6 where the shock velocity is shown as a function of particle velocity comparison for (a) epoxy-45Al and (b) epoxy-Al_2O_3

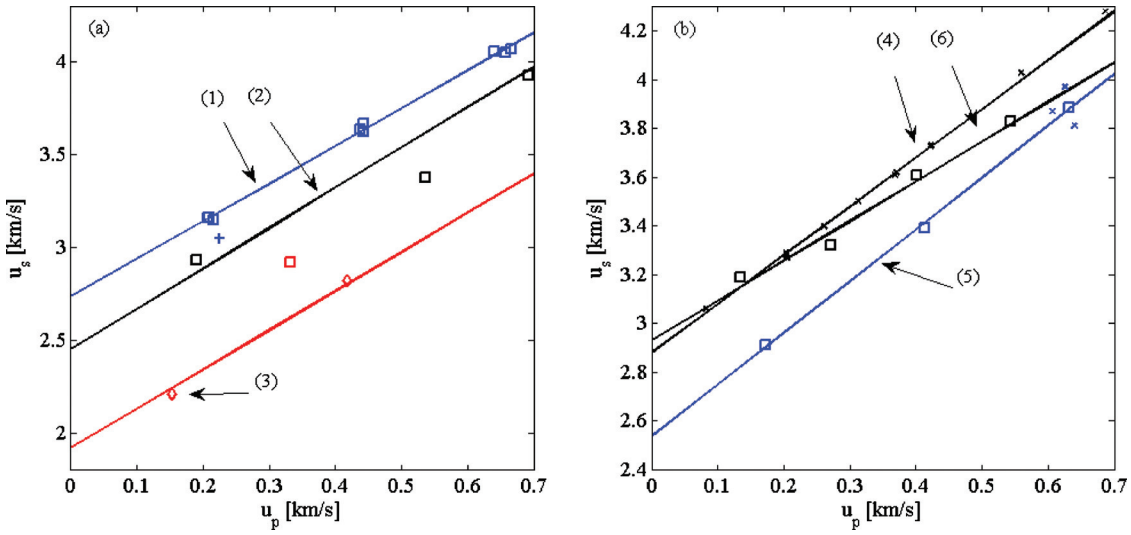

FIG. 6. (Color) Shock velocity vs particle velocity comparison for (a) epoxy-45Al and (b) epoxy-Al_2O_3 composites. (a) The black squares are the data points from Table III for epoxy-45Al. The (2) black line is the least-squares fit of this data: $U_s=2.45+2.18u_p$. There are three sets of blue squares that represent the results from taking each particle morphology (shown in Fig. 5) and subjecting it to impacts at 302, 622, and 960 m/s. The (1) blue line is a least-squares fit: $U_s=2.76+2.03u_p$. The blue "+" denotes an impact of the microstructure (a) using the Hugoniot data from Millett, Bourne, and Deas (Ref. 4). The blue circle denotes a simulation where the material properties are the same as for the blue squares, but a boundary layer interface was prescribed between the powder particles and the epoxy matrix. (b) The black squares are taken from Ref. 4. The blue squares are computed similarly to those in (a) but the results are taken from a digitized micrograph from Fig. 1 in Ref. 5 using the properties of epoxy and Al_2O_3. The blue line [denoted by (4)] shows the least-squares fit to this data: $U_s=2.54+2.12u_p$. the three blue "×" points show the results using the parameters from Ref. 6. The three points are taken from a "stitched" micrograph of epoxy-45Al where the Al particles are given the material properties of Al_2O_3.

TABLE V. Parameters for the material equation of state.

Material	EOS	ρ_0 (g/cc)	c_0 (km/s)	s_1	ν
Epon-828	Mie-Grüneisen	1.14	2.69	1.51	0.35
Al	Tabular	2.71	5.25	1.37	0.28
Al_2O_3	Mie-Grüneisen	3.98	7.93	1.20	0.28
Al 6061-T6	Mie-Grüneisen	2.71	5.22	1.37	0.28
W	Mie-Grüneisen	19.24	3.98	1.24	0.28

composites. The parameters used for the equation of state and strength models are shown in Tables V and VI.

In Fig. 6(a), the three black squares are the experimental data points from Table III for epoxy-45Al. The black line labeled (2) is the least-squares fit of this data: $U_s=2.45+2.18u_p$. There are three sets of three blue squares above the experimental line that represent the results from taking each particular particle morphology (shown in Fig. 4) and subjecting it to impacts at 302, 622, and 960 m/s. The simulations are repeated for each impact condition with different microstructures. The blue line labeled (1) is a least-squares fit of the numerical data points: $U_s=2.76+2.03u_p$. The blue "+" denotes an impact of the microstructure "A" using the epoxy Hugoniot data from.[4] Note that changing the c_0 and s_1 values for the epoxy only result in an averaged decrease in the shock speed (and slope which is not shown) for a particle velocity of 302 m/s. The two red diamonds are taken from the epoxy-Al–W data in Table III. The red line denoted by curve (3) is Eq. (4). The red square above this line is the simulated result using the microstructure from Fig. 8.

Figure 6(b) presents the shock speed (U_s) and particle speed (u_p) data from the fully loaded Al_2O_3 samples in Ref. 4 (black squares) and Ref. 3 (black "×" data). The blue squares are computed similarly to those in Fig. 5(a), but the results are taken from simulations using the particle morphology shown in Fig. 1 in Ref. 5, shown here in Fig. 7. The blue line [denoted by (4)] shows the least-squares fit to this data: $U_s=2.54+2.12u_p$. The three blue × points show the results using the epoxy parameters from Ref. 6. The three points are taken from a "stitched" micrograph of epoxy-45Al where the Al particles are given the material properties of Al_2O_3. The "stitched" micrograph was twice as long as those shown in Fig. 4 and the three points are U_s, u_p pairs measured at three different locations for lines of tracer particles placed at four different locations. The U_s, u_p pairs differ by about 1% in shock speed and in particle speed.

The results shown in Fig. 6(a) indicate that changing the particle morphology (e.g., see Fig. 5) does not result in an appreciable change in the U_s, u_p values. This is also true for simulations of epoxy-Al_2O_3 samples, as seen in Fig. 7, where the morphologies are drastically different not only in particle distribution, but size and shape. It is interesting that the slopes of the epoxy-45Al simulations match very well between simulations and experiments and that the experimental data for the epoxy-Al_2O_3 is between literature data depending on the material parameters used. It is most probable that uncertainties in the density and amount of fill of the epoxy-Al_2O_3 sample were the main cause of the discrepancy between the experiments and simulations. This is supported by the fact that, regardless of the type of material that is put into the epoxy (Al, Al_2O_3, etc.), it has been suggested that the epoxy matrix drives the response of the materials when the volume fraction of the fill material is low enough that particle-particle interactions do not have a strong effect.[4,6] The two red diamonds in Fig. 6(a) are taken from the epoxy-Al–W data in Table III. The red line denoted curve (3) is Eq. (4). The red square above this line is a simulated result using the microstructure from Fig. 8 impacted at 450 m/s resulting in values of $u_p=332$ m/s, $U_s=2.921$ km/s. The image from Fig. 1(e) was rotated 90° for the simulation in Fig. 8 to elongate the material in the direction of shock. The pressure distribution is shown in Fig. 8(b) at the stage where the shock has almost reached the bottom of the material and it is clear that the shock-front is nonuniform (the colors correspond to blue=0 GPa, and red=2 GPa). The W particles clearly disrupt the planarity of the shock front, but do not affect the slope of the U_s, u_p curve as indicated in Fig. 6(a) and from Eq. (4). The W particles are much less deformable than epoxy or the surrounding Al particles, which undergo much more bulk deformation along with the matrix.

V. CONCLUSIONS

This paper discussed equation of state experiments and complementary mesoscale simulations conducted on five epoxy-based particulate composites. Two of the composites contained only aluminum (35 and 45 vol %) and epoxy. The remaining three composites contained 35 vol % aluminum

TABLE VI. Parameters for material strength models. Al and Al_2O_3 used Johnson-Cook models built-in to CTH material libraries.

Material	Strength model	A (MPa)	B (MPa)	C	m	n	T_m (K)
Epon-828	Johnson-Cook	84	15	0.01	0.53	0.20	350
Al_2O_3	Johnson-Cook	3.98	7.93	1.20	0.28	0.60	2073
W	Johnson-Cook	1510	177	0.016	1	0.12	1748

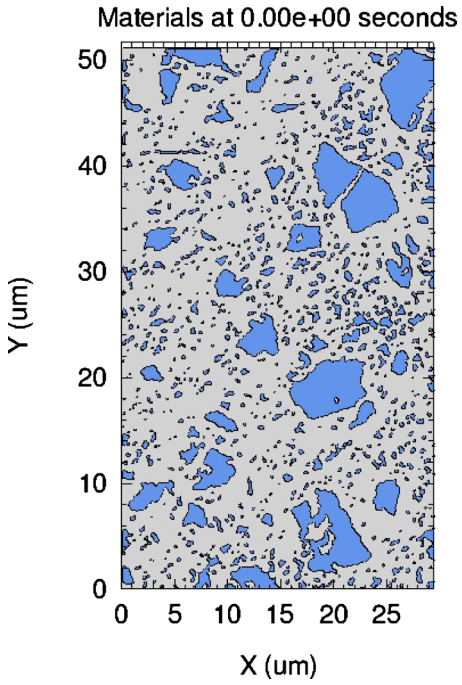

FIG. 7. (Color online) Digitized migrograph taken from Ref. 5. The computed density is 2.496 g/cm^3 which corresponds to 48 vol % of epoxy and 52% Al_2O_3.

with 10 vol % of an additional metal (copper, nickel, or tungsten) in an epoxy binder. The pressure and shock velocity of these epoxy-based composites were measured at impact velocities ranging from 300 to 960 m/s, using manganin gauges for stress and time of arrival measurements. Numerical simulations have been conducted comparing the epoxy-Al from this study with epoxy-Al_2O_3 previously published in the literature to investigate the effect of the material properties of the particulate. Additionally, a mesoscale simulation of epoxy-Al–W has been conducted to determine the effect of a second particulate phase.

The epoxy binder was found to drive the behavior of these materials. The experimental pressure versus time traces as measured with manganin pressure gauges showed little difference between the five materials studied. Comparing the shock velocity versus particle velocity curves for the five materials in this study as well as two from the literature revealed nominally linear behavior over the range studied and parallel linear fits varying only with sample density. Mesoscale numerical simulations of comparable formulations containing aluminum and alumina particulates demonstrated that the materials properties of the particulate did not greatly affect the shock behavior, excluding density effects. Simulations of epoxy-Al–W showed that the tungsten greatly affected the shock fron at the mesoscale, but this behavior is not manifested in the bulk shock behavior.

ACKNOWLEDGMENTS

The authors would like to acknowledge the help of Mr. Grant Rogerson (NSWC-IH) for assistance with the gas gun experiments. This research was funded by Air Force Research Laboratory.

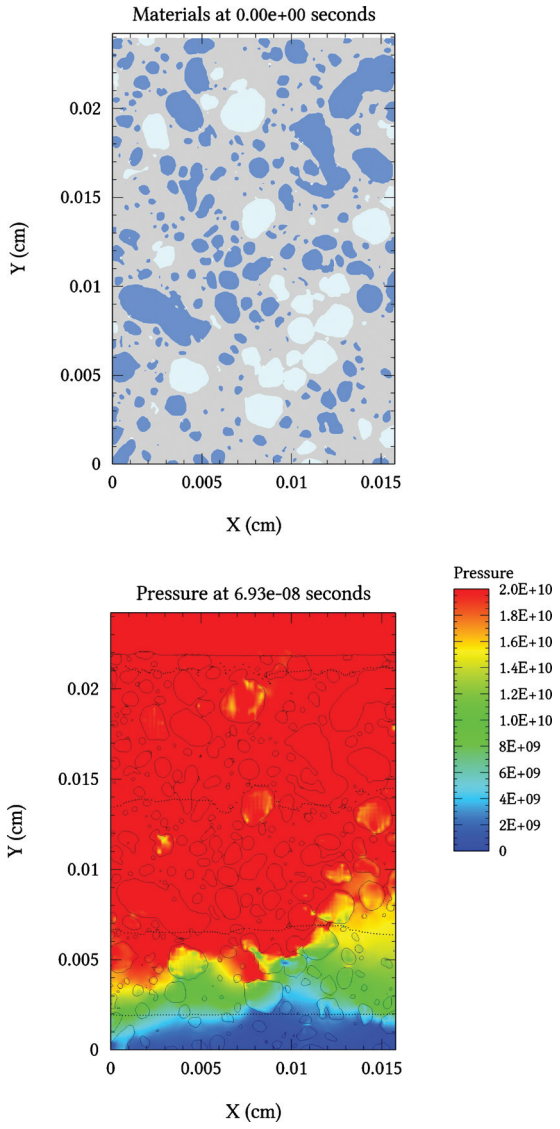

FIG. 8. (Color) Digitized micrograph of Fig. 1(e). The image was rotated 90° to elongate the material in the direction of shock. [U_{impact}=450 m/s, u_p=332 m/s, U_s=2.921 km/s, which is shown in Fig. 6(a)]. The pressure distribution is shown at the stage where the shock has almost reached the bottom of the material. The shock-front is nonuniform. The colors correspond to blue=0 GPa, and red=2 GPa. The temperature distribution is shown in the bottom part of the figure. The W particles are clearly distinguished from the soft Al particles, which undergo much more bulk deformation along with the matrix.

Opinions, interpretations, conclusions, and recommendations are those of the authors and not necessarily endorsed by the United States Air Force.

[1]D. E. Munson, R. R. Boade, and K. W. Schuler, J. Appl. Phys. **49**, 4797 (1978).
[2]M. U. Anderson, R. E. Setchell, and D. E. Cox, in *Shock Compression of Condensed Matter—1999*, edited by M. D. Furnish, L. C. Chhabildas, and R. S. Hixson (AIP, Melville, NY, 2000), pp. 551–554.
[3]R. E. Setchell and M. U. Anderson, J. Appl. Phys. **97**, 083518 (2005).
[4]J. C. F. Millettt, N. K. Bourne, and D. Deas, J. Phys. D: Appl. Phys. **38**, 930 (2005).
[5]R. E. Setchell, M. U. Anderson, and S. T. Montgomery, J. Appl. Phys. **101**, 083527 (2007).
[6]T. J. Vogler, C. S. Alexander, J. L. Wise, and S. T. Montgomery, J. Appl. Phys. **107**, 043520 (2010).
[7]L. Ferranti, Ph.D. dissertation, Georgia Institute of Technology, 2007.

[8]J. L. Jordan, L. Ferranti, R. A. Austin, R. D. Dick, J. R. Foley, N. N. Thadhani, D. L. McDowell, and D. J. Benson, J. Appl. Phys. **101**, 093520 (2007).
[9]J. L. Jordan, D. Dattelbaum, G. Sutherland, D. Richards, S. Sheffield, and R. Dick, J. Appl. Phys. **107**, 103528 (2010).
[10]A. Fraser, J. P. Borg, and J. L. Jordan, AIP Conf. Proc. **1195**, 61 (2009).
[11]W. J. Carter and S. P. Marsh, Hugoniot Equation of State of Polymers, Los Alamos National Laboratory Report No. LA-13006-MS, Los Alamos, NM, 1995.
[12]D. E. Munson and R. P. May, J. Appl. Phys. **43**, 962 (1972).
[13]J. C. F. Millettt, N. K. Bourne, and N. R. Barnes, J. Appl. Phys. **92**, 6590 (2002).
[14]E. B. Herbold, V. F. Nesterenko, D. J. Benson, J. Cai, K. S. Vecchio, F. Jiang, J. W. Addiss, S. M. Walley, and W. G. Proud, J. Appl. Phys. **104**, 103903 (2008).
[15]D. W. Richards, R. J. De Angelis, M. P. Kramer, J. W. House, D. A. Cunard, and D. P. Shea, Adv. X-Ray Anal. **47**, 351 (2004).
[16]R. L. Williamson, J. Appl. Phys. **68**, 1287 (1990).
[17]D. J. Benson, Modell. Simul. Mater. Sci. Eng. **2**, 535 (1994).
[18]M. R. Baer, C. A. Hall, R. L. Gustavsen, D. E. Hooks, and S. A. Sheffield, J. Appl. Phys. **101**, 034906 (2007).
[19]D. Eakins and N. N. Thadhani, J. Appl. Phys. **101**, 043508 (2007).
[20]J. M. McGlaun and S. L. Thompson, Int. J. Impact Eng. **10**, 351 (1990).
[21]J. P. Borg and T. J. Vogler, Int. J. Solids Struct. **45**, 1676 (2008).
[22]P. A. Conley and D. J. Benson, J. Appl. Phys. **86**, 6717 (1999).

DISTRIBUTION LIST
AFRL-RW-EG-TP-2012-003

*Defense Technical Info Center
8725 John J. Kingman Rd Ste 0944
Fort Belvoir VA 22060-6218

AFRL/RWME (6)
AFRL/RWOC-1 (STINFO Office)